Wound-Microenvironment Engineering

Subjects: Dermatology

Contributor: IRATXE MADARIETA

In patients with comorbidities, a large number of wounds become chronic, representing an overwhelming economic burden for healthcare systems. Engineering the microenvironment is a paramount trend to activate cells and burst-healing mechanisms. The extrusion bioprinting of advanced dressings was performed with novel composite bioinks made by blending adipose decellularized extracellular matrix with plasma and human dermal fibroblasts. Rheological and microstructural assessments of the composite hydrogels supported post-printing cell viability and proliferation over time.

bioink 3D bioprinting decellularized adipose extracellular matrix plasma platelet cytokines growth factors wound healing

1. Introduction

Skin is the first line of defense against many types of infections and diseases. Acute skin injuries, in healthy people, repair through a sequence of complex, constitutively active signaling pathways. However, in patients with comorbidities, a large number of wounds become chronic as they fail to repair within three months [1]. Diabetes, venous stasis, radiation or paralyses are common risk factors for complex wounds. In these patients, healing mechanisms fail to progress through the different stages and ulcers become stagnant. Wound chronicity, referred to as silent epidemic, is an overwhelming economic and medical burden for healthcare systems [2][3]. Common biological features of chronicity include uncontrolled inflammation and loss of the dermal cells' ability to respond to reparative stimuli [4].

The current standard of care (SOC) addresses several specific aspects related to wound etiology and involves the control of moisture in the wound bed through the careful personalized selection of dressings [5], which, theoretically, provide the conditions for proper cell/protein interactions committed to healing. However, closure rates in complex wounds are low [6]. On the other hand, cell-based wound dressings are commercialized and investigated to replace the current SOC [7]. Most cell-based dressings utilize a hydrogel scaffold upon which cells are seeded. There are three general categories, which include (1) amniotic and placental membranes (e.g., dehydrated (EpiFix®, Marietta, GA, USA), or cryopreserved (Grafix*, Osiris, Columbia, MD, USA)) [6]; (2) human allogeneic skin cells seeded in bovine type 1 collagen (e.g., OrCel® (Ortec International NY, USA), Apligraf®, Organogenesis Inc., Canton MA, USA) [8] or polyglactin mesh scaffold (Dermagraft®, Organogenesis Inc., Canton MA, USA) [9]; and (3) allogeneic fibrin patch with platelets and leukocytes (LeucoPatch® (Reapplix, Birkerød Denmark)) [10]. Their efficacy is better than the SOC, but there are still opportunities for refinement, as efficacies range between 31 and 50% of closure

[7]. In addition to the limited efficacy, higher upfront costs limit their integration in clinical practice [7]. The latter can be overcome by the adoption of novel manufacturing technologies, such as 3D bioprinting [11]. In particular, extrusion bioprinting is compatible with almost all hydrogels and can be easily scaled up to print at a reasonable cost [12][13][14].

Upgrading dressing manufacturing can help to meet the urgent clinical need created by ulcer chronicity, helping to mitigate obstacles to healing and, in doing so, restoring the skin barrier function in complex situations. Moreover, bioink customization can be achieved by the careful selection of autologous or homologous components following a biomimetic approach.

Even so, advanced dressings can fail to boost healing mechanisms because they encounter a hostile microenvironment rich in inflammatory cytokines and enzymes, such as collagenase, gelatinases, stromelysins and cell-membrane-associated MMPs (Matrix Metalloproteinases), which contribute to the rapid clearance of growth factors and cytokines in the wound area and are detrimental for cell viability. Therefore, engineering the microenvironment has been regarded as a paramount trend to enhance cell survival and burst-healing mechanisms by the constant release and diffusion of signaling proteins [15].

Several novel bioinks for skin engineering have been developed in the past two years [16]. However, existing bioinks cannot meet the complex needs of difficult-to-heal wounds [11]. An ideal scenario would present the cells within advanced dressings in a natural microenvironment that exhibits similar characteristics to a healing tissue. In this work, biomimetic hydrogels formulated as smart bioinks for manufacturing new modalities of advanced dressings were created by blending porcine decellularized adipose matrix (pDAM2) [17] and alginate with platelets and plasma growth factors at two concentrations and human dermal cells. The proteomic analysis of pDAM2 confirmed that several proteins, specifically, collagens, proteoglycans, glycoproteins and affiliated proteins, were preserved. The complete proteomic analysis of pDAM2 material has been previously reported by the team [17]. Besides, pDAM2 hydrogels can provide mechanical support to enhance cell attachment and modulate cell behavior, regulating cell phenotype and function, as well as infection. Actually, since the Egyptians [18], bandages made with grease from animal fat have been used as a barrier to bacteria to treat battle injuries [19]. On the other hand, by adding PRP (platelet-rich plasma) to bioink (dressing), researchers provided active biological molecules to drive cell activities towards the enrichment of healing mechanisms. Finally, by blending pDAM2, plasma and human dermal fibroblasts, their advanced dressings could mimic cell-to-matrix and cell-to-environment interactions, paramount for physiologically relevant cell functions.

Within the clinical context, according to a recent meta-analysis, PRP-assisted fat grafting is effective in soft-tissue augmentation [20]. In particular, diabetic foot ulcers treated with fat and PRP showed increased vessel density and graft survival [21]. Although fat combined with PPP has been poorly investigated in humans, research in nude mice revealed that both PRP and PPP enhanced fat-graft survival, although PRP had stronger angiogenic effects [22].

2. Rheological and Microstructural Properties of the Composite Bioinks

For extrusion-based 3D printing, the material must have adequate zero-shear viscosity and shear-thinning properties to extrude smoothly through a narrow nozzle. The pDAM2: PRP/ALG and pDAM2: PPP/ALG bioinks showed shear-thinning behavior in a shear-stress range of 1–1000 s^{-1}—viscosity is a decreasing function of the shear rate. Viscosity values at shear rates of 1 s^{-1} for the pDAM2: PRP/ALG and pDAM2: PPP/ALG hybrid bioinks were measured at 6.30 and 8.27 Pas, respectively. The viscosity of the hybrid bioinks showed medium values compared with raw bioinks DAM2, PRP/ALG and PPP/ALG (**Figure 1**A).

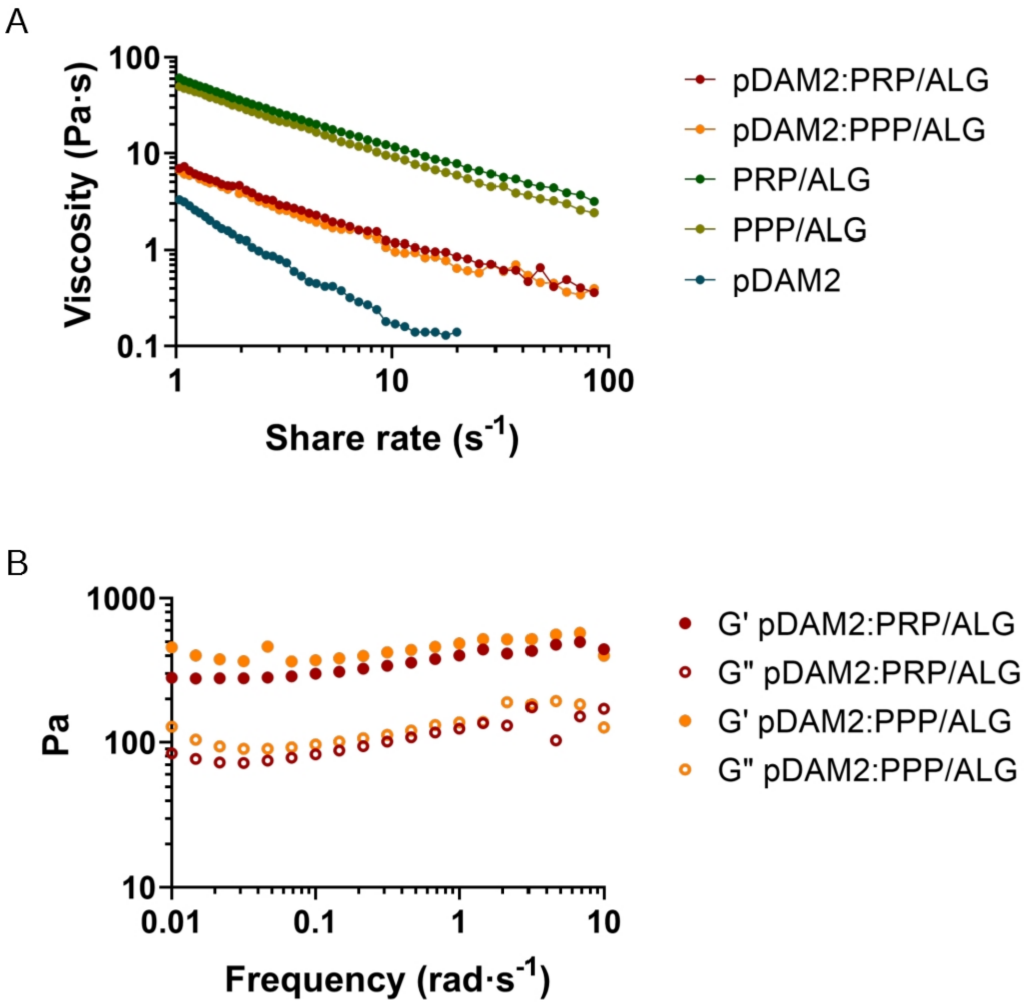

Figure 1. Rheological behavior: (**A**) flow curves of pDAM2: PRP/ALG and pDAM2: PPP/ALG inks and the individual components; (**B**) dynamic moduli at varying frequency at 37 °C of hydrogels (storage and loss moduli measured by frequency sweep tests of pDAM2: PRP/ALG and pDAM2: PPP/ALG inks).

Because good fluidity during bioink extrusion and gelling ability just after deposition are essential for bioprinting, the rheological behavior of the hydrogels was investigated. When the rheological properties were measured under oscillating conditions after gelification, the hybrid hydrogels exhibited gel-like properties, with the storage modulus (G′) being higher than the loss modulus (G″) (**Figure 1**B). Thus, after gelation, the hydrogels retained their shape and form, which is a prerequisite for the fabrication of 3D-bioprinted dressings. The pDAM2 hydrogel showed the lowest storage modulus; moreover, the PRP/ALG and PPP/ALG hydrogels exhibited a similar rheological profile in

terms of storage and loss modulus and revealed larger storage moduli than the hybrid hydrogels (pDAM2:PRP/ALG, pDAM2:PPP/ALG).

Scanning electron microscopy of the pDAM2 hydrogels showed a randomly oriented fibrillar structure, with an average fiber diameter of less than 100 nm and interconnecting pores. The PRP/ALG and PPP/ALG hydrogels exhibited microstructures with many irregular aggregates. However, the images of the pDAM2: PRP/ALG and pDAM2: PPP/ALG hybrid hydrogels revealed that those aggregates were covered by the fibrillar structure of the pDAM2 hydrogels (**Figure 2**).

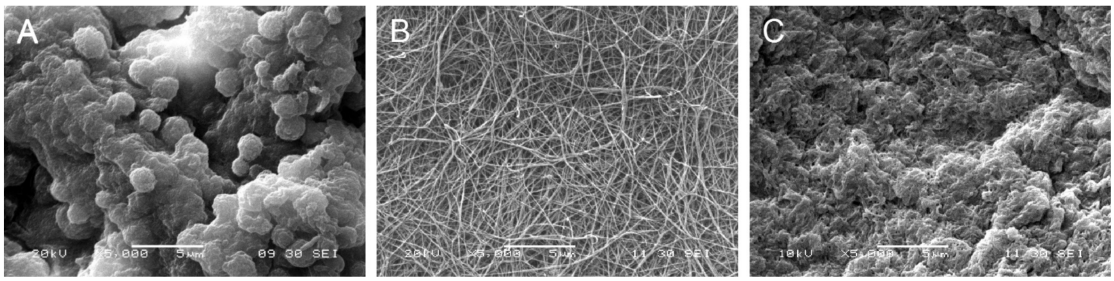

Figure 2. Scanning electron microscopy (SEM) images of: (**A**) PRP/ALG, (**B**) pDAM2 and (**C**) pDAM2: PRP/ALG.

Regarding the advantages in bioprinting processes, the behavior of the hydrogel blends (pDAM2: PRP/ALG and pDAM2: PPP/ALG) was individually superior to the plasma bioinks and allowed us to reduce the diameter of the extrusion needle (from 20 G to 22 G), improving filament homogeneity, without detrimental consequences in terms of cell viability.

Before bioprinting, cytocompatibility was assessed. The HDFs encapsulated within these constructs were metabolically active in the formulation of both hydrogels. Both blends, pDAM2: PRP/ALG and pDAM2: PPP/ALG, stimulated higher metabolic activity than the single pDAM2 hydrogel.

3. Three-Dimensional Bioprinting Procedure, Post-Printing Cell Viability and Proliferation in Wound Dressings

Following the methodology described before [23], proper 3D-printing resolution and dispensing uniformity were achieved with both pDAM2:PRP/ALG and pDAM2:PPP/ALG bioinks, obtaining advanced wound dressings with high reproducibility. This was due to filament uniformity during extrusion and maintenance of the construct stability with 100% infill. Further structural integrity of the dressings was achieved by physical cross-linking using CaCl2 (**Figure 3**A). The results showed a high number of HDF cells viable after bioprinting with pDAM2: PRP/ALG and pDAM2: PPP/ALG (**Figure 3**B,C), whereas a very low number of dead cells was observed in all tested dressings. Staining for cell viability and cell density revealed that both bioink modalities had comparable cytocompatibility and bioactivity to promote cell growth. Changes in cell density and morphology over time confirmed that the bioinks allowed cells to adhere and grow in an ideal 3D microenvironment.

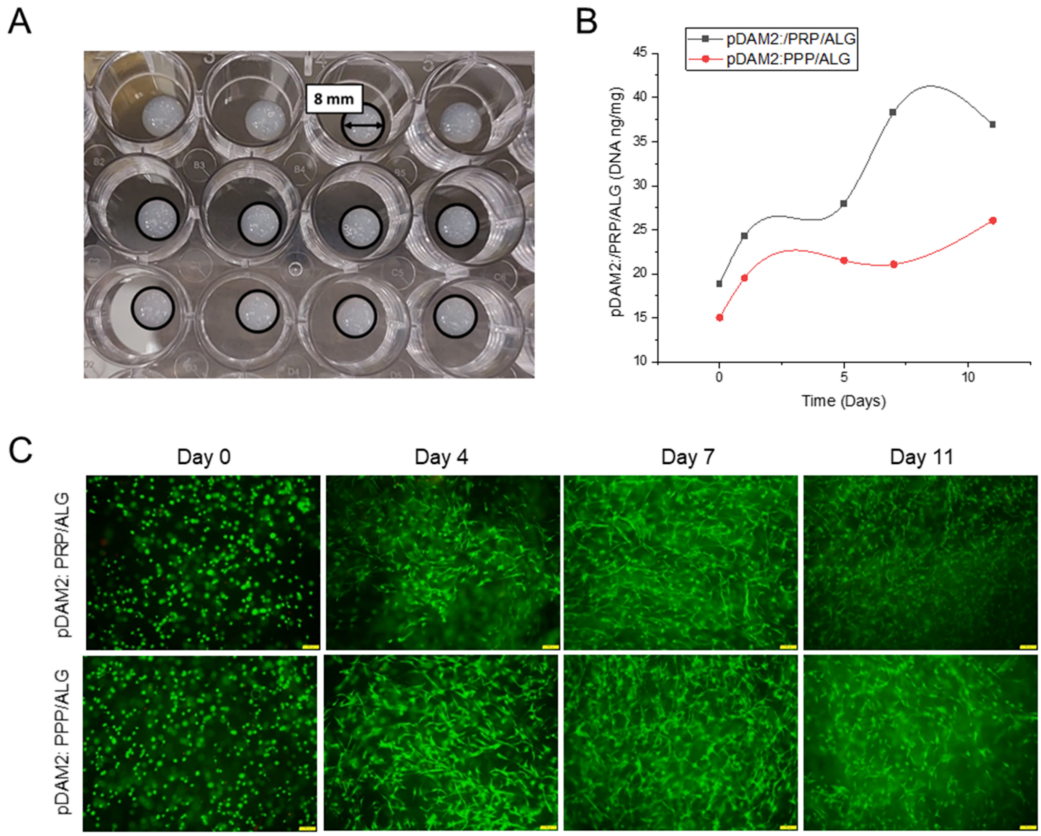

Figure 3. (**A**) Macroscopic image of cell-laden constructs bioprinted on 24-well plates. (**B**) HDF proliferation (DNA ng/mg construct) within a period of 11 days of culture. (**C**) HDF viability at 0, 4, 7 and 11 days of culture after bioprinting with pDAM2:PRP/ALG and pDAM2:PPP/ALG. Green corresponds to calcein-AM staining of life cells and red corresponds to Propidium iodide staining of dead cells (scale bar = 100 µm).

4. Expression of Extracellular Matrix Proteins by Embedded Dermal Fibroblasts

The HDFs embedded within the advanced dressings showed high expression of FN and moderate expression of COL1A1, COL1A2 and COL3A1 relative to GAPDH. On the other hand, the expression of COL4A1 and COL4A2 was low and ELN expression was under the detection limits. Repeated measurements of gene expression showed steady levels of expression, without statistically significant changes over time in any of the analyzed molecules (**Figure 4**).

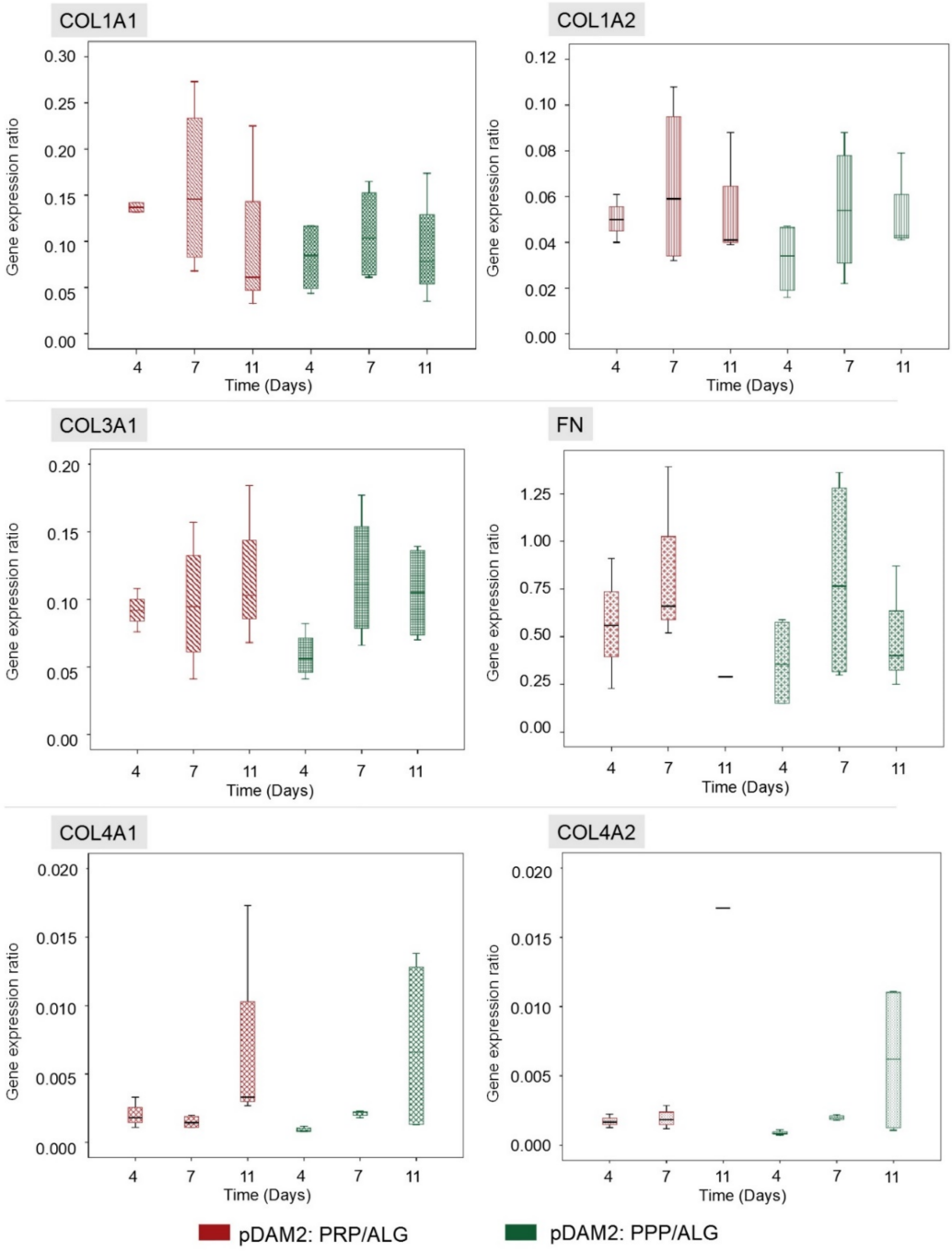

Figure 4. HDFs embedded within both modalities of advanced dressings showed moderate expression of COL1A1, COL1A2 and COL3A1 relative to GAPDH, without variations over time. The expression of fibronectin was high in both dressing types (RNA from the 11-day construct was lost), whereas the expression of COL4A1 and COL4A2 was low. There were no significant changes in gene expression over time and no differences between the two dressing modalities.

5. Paracrine Potential of Wound Dressings: Signaling Protein Expression over Time

To evaluate the effects of manufactured dressings on the wound microenvironment, researchers investigated the release of healing signaling molecules over time. Fibroblasts embedded in either pDAM2: PRP/ALG or pDAM2: PPP/ALG synthesized and released wound-healing cytokines over 11 days; protein concentrations were normalized with protein data at 1 h. In doing so, they obtained folds relative to one-hour cultures. Using core IPAs, researchers found that the “wound healing” canonical pathway was significantly enriched in their data. **Figure 5**A depicts important molecules in this pathway. Z-score values predicted that wound healing was activated over time by the molecules released from the construct (**Figure 5**B). The Z-score increased over time for the pDAM2: PRP/ALG dressings (4 d, Z = 0.365; 7 d, Z = 1.616; 11 d, Z = 3.413), while the maximum Z-score for pDAM2: PPP/ALG was achieved at 7 d (4 d, Z = 1.061; 7 d, Z = 2.611; 11 d, Z = 1.257). In parallel, the Z-score for paracrine activation of cell signaling and viability displayed a similar pattern of variation, with differences between both dressings (**Figure 5**C).

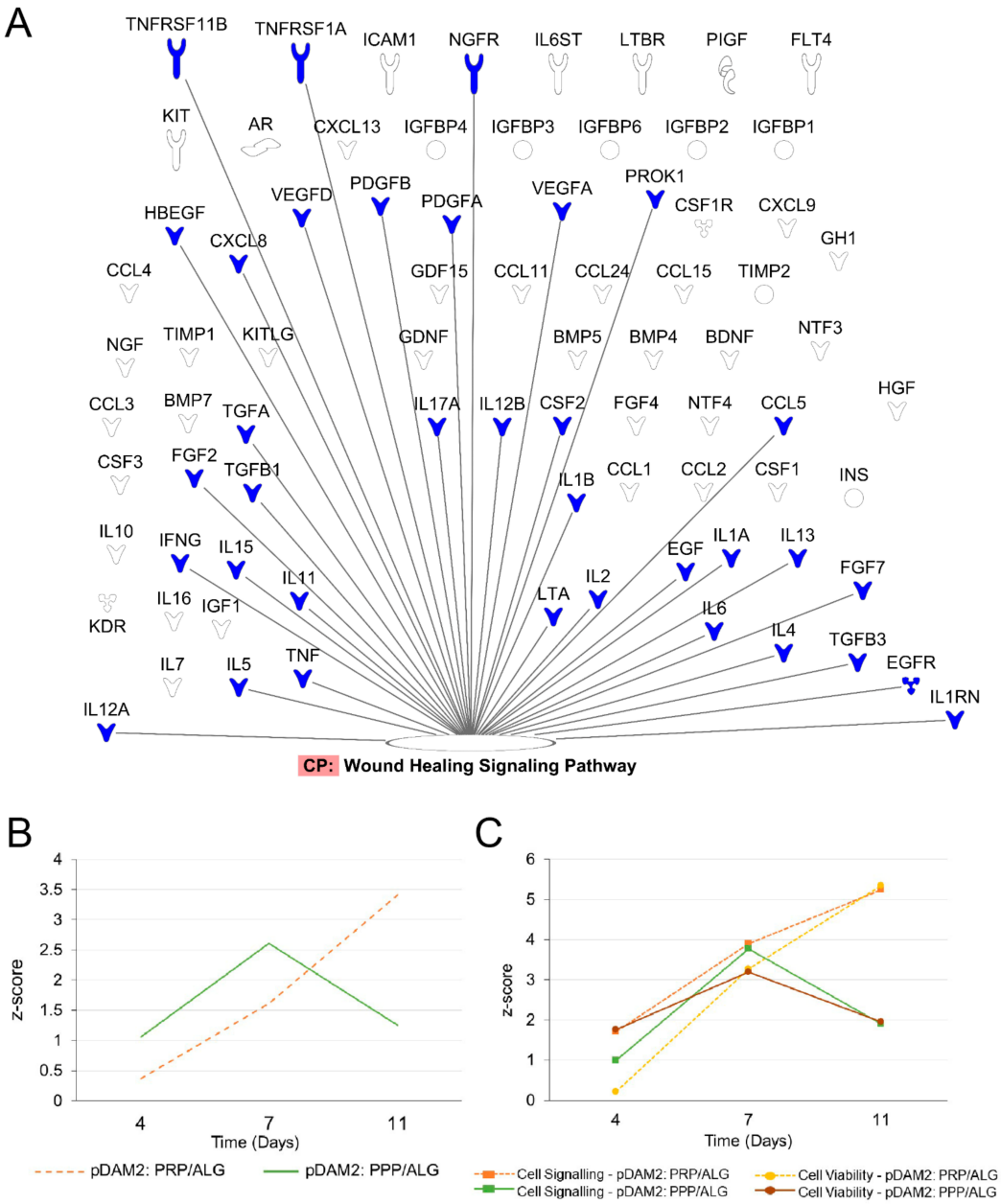

Figure 5. Signaling pathways enriched in the data obtained from the analysis of the conditioned media. (**A**) Signaling molecules synthesized by encapsulated cells over time that were involved in the wound-healing signaling pathway. (**B**,**C**) pattern of Z-score outcome over time predicting activation of the wound-healing signaling pathway (**B**), cell signaling and cell viability (**C**).

To confirm the predictions obtained by the IPA algorithms, researchers used ELISAs to perform individual assessments of relevant cytokines involved in cell signaling and modulation of inflammation and angiogenesis. IL-8 is a pleiotropic interleukin involved in cell activation and movement; both modalities of advanced dressings showed significant synthesis and release of IL-8 over time ($p < 0.001$). Maximum release was achieved after 4 days without additional synthesis from day 4 to day 11 in any of the bioink variants ($p \leq 0.001$) (**Figure 6**A). On the other hand, MCP-1, also known as CCL-2, was not detected in acellular scaffolds at any time point (**Figure 6**B). However, the HDFs embedded within the pDAM2:PRP/ALG dressings synthesized increasing concentrations of MCP-1 over time ($p < 0.001$); maximum concentrations were achieved after 11 days of culture, representing a 70-fold increase compared with 1-hour concentrations (26.72 ± 1.14 ng/mL at 11 days and 0.372 ± 0.008 ng/mL at 1 hour). Instead, the pDAM2: PPP/ALG dressings released MCP-1 after four days but did not show additional synthesis over time. The amount of MCP1 released by the pDAM2: PRP/ALG dressings was significantly higher at 11 days (26.716 ± 1.14 ng/mL versus 8.92 ± 0.52 ng/mL; $p < 0.001$).

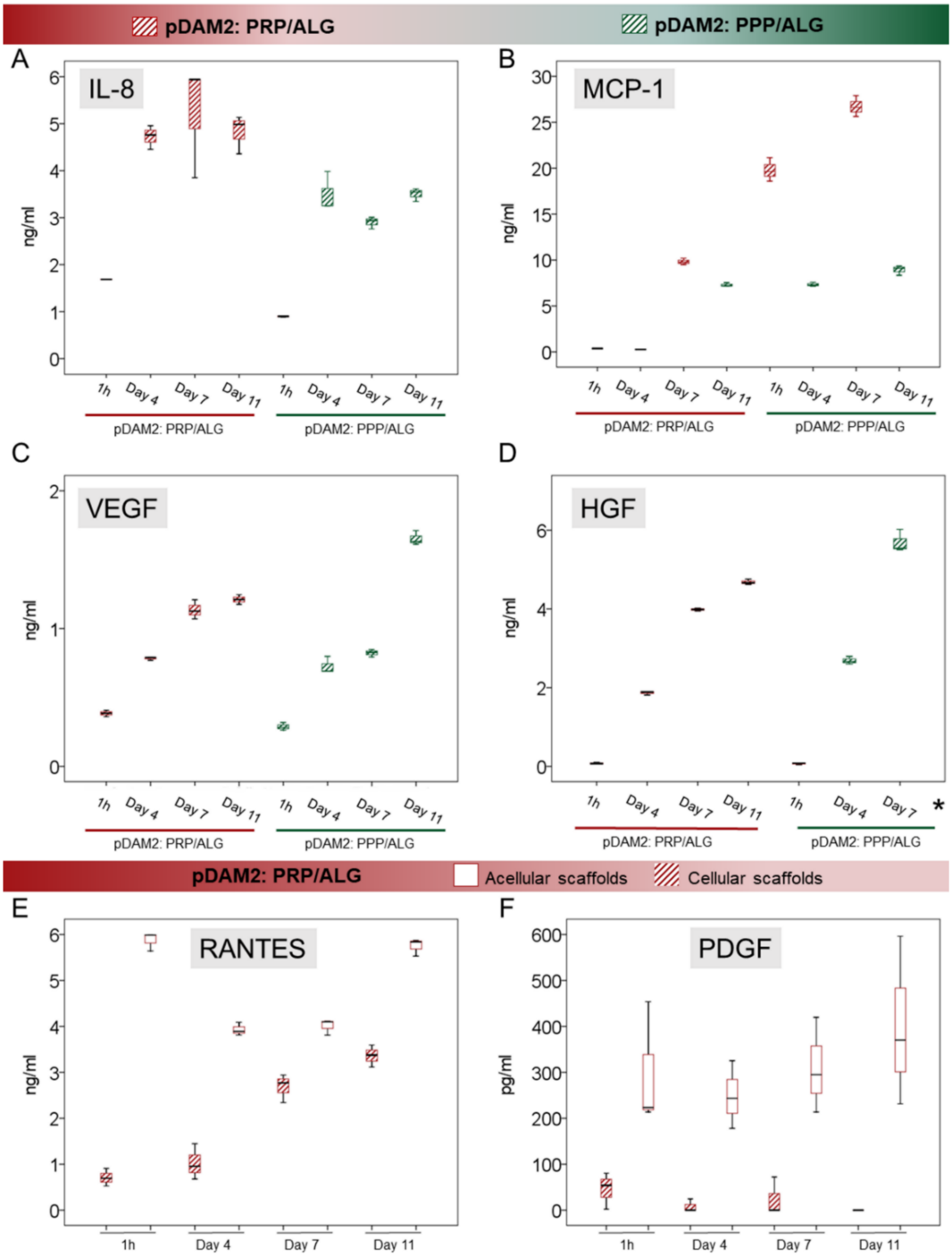

Figure 6. (**A**–**D**) Box plots show the median and 25–75 percentiles of relevant signaling cytokines involved in the modulation of inflammation (IL-8 and MCP-1, (**A**) and (**B**), respectively) and in angiogenesis (VEGF and HGF, (**C**) and (**D**), respectively) measured by ELISA in the conditioned media harvested over time. * Mean HGF concentration at Day 11 was 98,198 ± 3815 ng/mL (not shown in the graph). (**E**,**F**) RANTES and PDGF-BB released from the PRP component in the pDAM2: PRP/ALG dressings (as shown by acellular scaffolds cultured in the same conditions) were used up by embedded cells.

Researchers quantified VEGF and HGF as an index of angiogenesis. There was a significant synthesis of VEGF and HGF by both advanced dressings, i.e., manufactured with either the pDAM2: PRP/ALG or pDAM2: PPP/ALG

bioink, with $p < 0.001$ for both dressings and both proteins. Of note, cells within the pDAM2: PPP/ALG dressings released higher concentrations of VEGF and HGF after 7 and 11 days (**Figure 6**C,D).

On the other hand, researchers measured RANTES (CCL5) and PDGF, which are abundant platelet proteins, here provided by the PRP component of the prepared bioink. The pDAM2: PPP/ALG constructs did not show any synthesis/secretion of RANTES and PDGF-BB. Remarkably, RANTES and PDGF-BB released from the PRP dressings without cells showed higher concentrations than those released by the constructs with cells, pointing out protein consumption by the embedded fibroblasts.

6. Indirect Co-Cultures: Dermal-Cell Proliferation

The conditioned media harvested over time from the two modalities of advanced dressings (differing in platelet number) stimulated human-dermal-cell proliferation, as revealed by indirect co-cultures. The media harvested from the bioprinted constructs manufactured without cells was used as control. The conditioned media from cells within the pDAM2: PRP/ALG dressings had a more-potent proliferating activity than the conditioned media from the pDAM2: PPP/ALG dressings ($p = 0.001$) (**Figure 7**). Although the proliferation rate was optimal for both dressing modalities, those manufactured with pDAM2: PRP/ALG reached higher proliferation rates with the conditioned media harvested after 7–11 days of in vitro maturation.

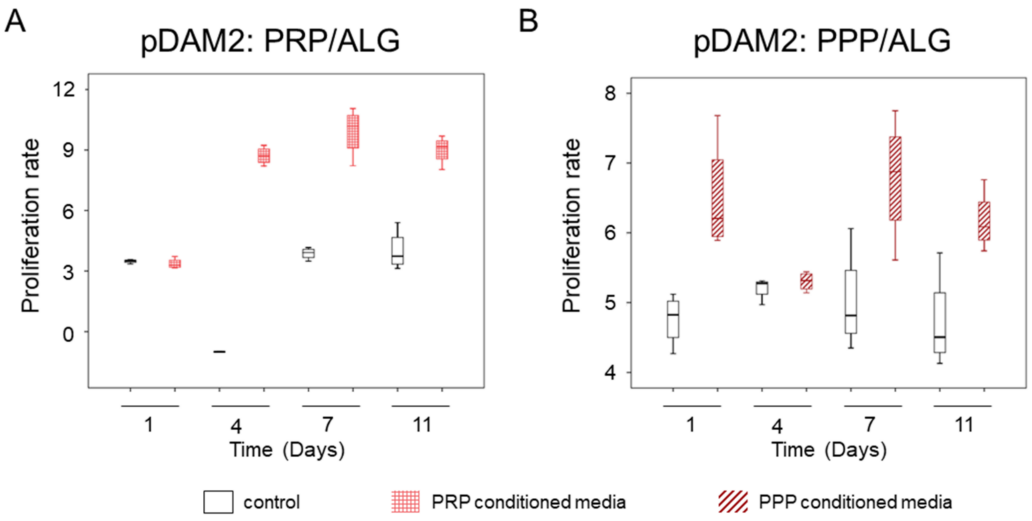

Figure 7. (**A**) Proliferative effect of conditioned media harvested from advanced dressings manufactured with PRP. (**B**) Proliferative effect of conditioned media harvested from advanced dressings manufactured with PPP.

References

1. Martin, P.; Nunan, R. Cellular and molecular mechanisms of repair in acute and chronic wound healing. Br. J. Dermatol. 2015, 173, 370–378.

2. Guest, J.F.; Ayoub, N.; McIlwraith, T.; Uchegbu, I.; Gerrish, A.; Weidlich, D.; Vowden, K.; Vowden, P. Health economic burden that different wound types impose on the UK's National Health Service. Int. Wound J. 2017, 14, 322–330.
3. Olsson, M.; Järbrink, K.; Divakar, U.; Bajpai, R.; Upton, Z.; Schmidtchen, A.; Car, J. The humanistic and economic burden of chronic wounds: A systematic review. Wound Repair Regen. 2019, 27, 114–125.
4. Berlanga-Acosta, J.A.; Guillén-Nieto, G.E.; Rodríguez-Rodríguez, N.; Mendoza-Mari, Y.; Bringas-Vega, M.L.; Berlanga-Saez, J.O.; del Barco Herrera, D.G.; Martinez-Jimenez, I.; Hernandez-Gutierrez, S.; Valdés-Sosa, P.A. Cellular Senescence as the Pathogenic Hub of Diabetes-Related Wound Chronicity. Front. Endocrinol. 2020, 11, 661.
5. Evidence-Based Clinical Practice Guideline: Chronic Wounds of the Lower Extremity. Available online: www.plasticsurgery.org (accessed on 31 January 2022).
6. Gibbons, G.W. Grafix®, a Cryopreserved Placental Membrane, for the Treatment of Chronic/Stalled Wounds. Adv. Wound Care 2015, 4, 534.
7. Pourmoussa, A.; Gardner, D.J.; Johnson, M.B.; Wong, A.K. An update and review of cell-based wound dressings and their integration into clinical practice. Ann. Transl. Med. 2016, 4, 457.
8. Still, J.; Glat, P.; Silverstein, P.; Griswold, J.; Mozingo, D. The use of a collagen sponge/living cell composite material to treat donor sites in burn patients. Burns 2003, 29, 837–841.
9. Hart, C.E.; Loewen-Rodriguez, A.; Lessem, J. Dermagraft: Use in the Treatment of Chronic Wounds. Adv. Wound Care 2012, 1, 138–141.
10. Game, F.; Jeffcoate, W.; Tarnow, L.; Jacobsen, J.L.; Whitham, D.J.; Harrison, E.F.; Ellender, S.J.; Fitzsimmons, D.; Löndahl, M.; Dhatariya, K.; et al. LeucoPatch system for the management of hard-to-heal diabetic foot ulcers in the UK, Denmark, and Sweden: An observer-masked, randomised controlled trial. Lancet Diabetes Endocrinol. 2018, 6, 870–878.
11. Perez-Valle, A.; Del Amo, C.; Andia, I. Overview of current advances in extrusion bioprinting for skin applications. Int. J. Mol. Sci. 2020, 21, 6679.
12. Tan, C.T.; Liang, K.; Ngo, Z.H.; Dube, C.T.; Lim, C.Y. Application of 3D Bioprinting Technologies to the Management and Treatment of Diabetic Foot Ulcers. Biomedicines 2020, 8, 441.
13. Fan, F.; Saha, S.; Hanjaya-Putra, D. Biomimetic Hydrogels to Promote Wound Healing. Front. Bioeng. Biotechnol. 2021, 9, 773.
14. Cui, X.; Li, J.; Hartanto, Y.; Durham, M.; Tang, J.; Zhang, H.; Hooper, G.; Lim, K.; Woodfield, T. Advances in Extrusion 3D Bioprinting: A Focus on Multicomponent Hydrogel-Based Bioinks. Adv. Healthc. Mater. 2020, 9, 1901648.

15. Scull, G.; Brown, A.C. Development of Novel Microenvironments for Promoting Enhanced Wound Healing. Curr. Tissue Microenviron. Rep. 2020, 1, 73–87.
16. Chang, P.; Li, S.; Sun, Q.; Guo, K.; Wang, H.; Li, S.; Zhang, L.; Xie, Y.; Zheng, X.; Liu, Y. Large full-thickness wounded skin regeneration using 3D-printed elastic scaffold with minimal functional unit of skin. J. Tissue Eng. 2022, 13, 204173142110630.
17. Cicuéndez, M.; Casarrubios, L.; Feito, M.J.; Madarieta, I.; Garcia-Urkia, N.; Murua, O.; Olalde, B.; Briz, N.; Diez-Orejas, R.; Portolés, M.T. Effects of Human and Porcine Adipose Extracellular Matrices Decellularized by Enzymatic or Chemical Methods on Macrophage Polarization and Immunocompetence. Int. J. Mol. Sci. 2021, 22, 3847.
18. Shah, J.B. The history of wound care. J. Am. Col. Certif. Wound Spec. 2011, 3, 65–66.
19. Human Fat Was Once a Medicine With a Black Market—The Atlantic. Available online: https://www.theatlantic.com/health/archive/2019/05/human-fat-was-once-medicine-black-market/590164/ (accessed on 1 February 2022).
20. Wu, M.; Karvar, M.; Liu, Q.; Orgill, D.P.; Panayi, A.C. Comparison of Conventional and Platelet-Rich Plasma-Assisted Fat Grafting: A Systematic Review and Meta-analysis. J. Plast. Reconstr. Aesthetic Surg. 2021, 74, 2821–2830.
21. Nolan, G.S.; Smith, O.J.; Heavey, S.; Jell, G.; Mosahebi, A. Histological analysis of fat grafting with platelet-rich plasma for diabetic foot ulcers-A randomised controlled trial. Int. Wound J. 2022, 19, 389–398.
22. Li, J.; Chen, W.; Shi, X.; Yu, P. Comparison of the Effects of Repeated Applications of Platelet-Rich Plasma versus Platelet-Poor Plasma on Fat Graft Survival in Nude Mice. Biomed Res. Int. 2021, 2021, 6613783.
23. Del Amo, C.; Perez-Valle, A.; Perez-Garrastachu, M.; Jauregui, I.; Andollo, N.; Arluzea, J.; Guerrero, P.; de la Caba, K.; Andia, I. Plasma-Based Bioinks for Extrusion Bioprinting of Advanced Dressings. Biomedicines 2021, 9, 1023.